The EMBO Journal Vol.18 No.6 pp.1492–1505, 1999

The Hdj-2/Hsc70 chaperone pair facilitates early steps in CFTR biogenesis

Geoffrey C.Meacham[1], Zhen Lu[1], Scott King[2,3], Eric Sorscher[2,3], Albert Tousson[1,3] and Douglas M.Cyr[1,3,4]

Departments of [1]Cell Biology, [2]Physiology and the [3]Gregory Fleming James Cystic Fibrosis Center, School of Medicine and Dentistry, University of Alabama Medical Center, Birmingham, AL 35209, USA

[4]Corresponding author
e-mail: DCYR@CELLBIO.BHS.UAB.EDU

The cystic fibrosis transmembrane conductance regulator (CFTR) is a chloride ion channel constructed from two membrane-spanning domains (MSDs), two nucleotide-binding domains (NBD) and a regulatory (R) domain. The NBDs and R-domain are cytosolic and how they are assembled with the MSDs to achieve the native CFTR structure is not clear. Human DnaJ 2 (Hdj-2) is a co-chaperone of heat shock cognate 70 (Hsc70) which is localized to the cytosolic face of the ER. Whether Hdj-2 directs Hsc70 to facilitate the assembly of cytosolic regions on CFTR was investigated. We report that immature ER forms of CFTR and ΔF508 CFTR can be isolated in complexes with Hdj-2 and Hsc70. The ΔF508 mutation is localized in NBD1 and causes the CFTR to misfold. Levels of complex formation between ΔF508 CFTR and Hdj-2/Hsp70 were ~2-fold higher than those with CFTR. The earliest stage at which Hdj-2/Hsc70 could bind CFTR translation intermediates coincided with the expression of NBD1 in the cytosol. Interestingly, complex formation between Hdj-2 and nascent CFTR was greatly reduced after expression of the R-domain. In experiments with purified components, Hdj-2 and Hsc70 acted synergistically to suppress NBD1 aggregation. Collectively, these data suggest that Hdj-2 and Hsc70 facilitate early steps in CFTR assembly. A putative step in the CFTR folding pathway catalyzed by Hdj-2/Hsc70 is the formation of an intramolecular NBD1–R-domain complex. Whether this step is defective in the biogenesis of ΔF508 CFTR will be discussed.
Keywords: cystic fibrosis transmembrane conductance regulator/DnaJ/Hsp70/membrane protein biogenesis/protein folding

Introduction

How cytosolic regions of polytopic membrane proteins fold and assemble into native conformations is a fundamental question in biology. Biogenesis of multiple domain proteins is proposed to proceed via a sequential pathway with sub-domain folding initiating co-translationally and final assembly occurring after completion of synthesis (Fedorov and Baldwin, 1997; Netzer and Hartl, 1997). The folding of extracellular domains on membrane proteins in the ER has been the subject of intense study in recent years and numerous lumenal protein-folding catalysts which facilitate this process have been identified (Hurtley and Helenius, 1989; Gaut and Hendershot, 1993). However, many membrane proteins possess large sub-domains which are exposed to the cytosol and how the cell facilitates the folding/assembly of this class of polypeptide is not clear. For instance, little information is available to describe steps in the assembly pathway of ATP binding cassette proteins (Higgins, 1992) such as the cystic fibrosis transmembrane conductance regulator (CFTR) (Riordan *et al.*, 1989).

CFTR is a 140 kDa glycoprotein which contains two membrane-spanning domains (MSDs) and two large cytosolic regions (Riordan *et al*., 1989). The first cytosolic region of CFTR is the size of an average protein (~500 amino acid residues) and contains two sub-domains, a nucleotide-binding domain (NBD1) and a regulatory (R) domain. The second cytoplasmic region is separated from the first by MSD2 and contains an additional nucleotide-binding fold termed NBD2. The sub-domains of CFTR assemble to form a channel which is proposed to conduct small anions, water and ATP (Anderson *et al*., 1991). The phosphorylation state of the R-domain controls the channel activity of CFTR via a mechanism which involves modulation of NBD1's affinity for ATP (Winter and Welsh, 1997).

Assembly of the CFTR channel initiates with its synthesis and folding in the ER and it can attain its native conformation in this cellular location (Pasyk and Foskett, 1995). Numerous reports indicate that early steps in CFTR biogenesis are inefficient. The majority of CFTR and almost all of ΔF508 CFTR, the mutant identified in most cystic fibrosis cases, never reach the plasma membrane and are degraded in a pre-Golgi compartment via a pathway which involves the proteasome (Yang *et al*., 1993; Lukacs *et al*., 1994; Ward and Kopito, 1994; Jensen *et al*., 1995; Ward *et al*., 1995). Inefficiencies in ΔF508 CFTR processing can be ameliorated by the growth of cells at low temperature (Denning *et al*., 1992) or by addition of chemical chaperones to cell culture media (Brown *et al*., 1996; Sato *et al*., 1996). Thus, folding/assembly defects appear to cause nascent ΔF508 CFTR to be diverted from the biosynthetic pathway to degradative pathways (Denning *et al*., 1992). Defective biogenesis of ΔF508 CFTR contributes to the clinical pathology of cystic fibrosis (Welsh and Ostedgaard, 1998).

The pathway and components that facilitate the folding and assembly of CFTR are currently being identified. A fragment of CFTR that contains MSD1, NBD1 and the R-domain is functionally active, which suggests that these domains can fold and assemble independently of MSD2 and NBD2 (Sheppard *et al*., 1994; Xiong *et al*., 1997; Schwiebert *et al*., 1998). However, studies on the

processing of the many CFTR mutants identified indicate that regions within MSD2 and NBD2 are also critical for proper folding and assembly (Welsh and Smith, 1993; Welsh and Ostedgaard, 1998). Thus, regions within the N- and C-terminus must interact in order for CFTR to form a stable ion channel.

Molecular chaperones localized in the ER lumen (calnexin) and cytosol (Hsp70) have been observed to transiently interact with immature CFTR (Yang *et al*., 1993; Pind *et al*., 1994). ΔF508 CFTR–Hsp70 and ΔF508 CFTR–calnexin complexes have a longer half-life than similar complexes with CFTR. Therefore Hsp70 and calnexin may function in the 'quality control' system which recognizes misfolded ER proteins (Yang *et al*., 1993; Pind *et al*., 1994). CFTR was also detected in complexes with Hsp70 and calnexin, therefore these chaperones may also function to facilitate normal folding of this membrane protein. Indeed, Hsp70 was recently shown to promote the folding of a CFTR fragment that corresponds to NBD1 (Strickland *et al*., 1997).

To facilitate protein folding, Hsp70 must interact with co-chaperone proteins that regulate its ability to bind and release non-native regions of proteins (Cyr, 1997; Frydman and Hohfeld, 1997; Hohfeld and Jentsch, 1997; Takayama *et al*., 1997). A major class of Hsp70 co-chaperone proteins are members of the Hsp40 (DnaJ-related) family (Cyr *et al*., 1994) whose progenitor is *Escherichia coli* DnaJ (Georgopoulos *et al*., 1980; Zylicz *et al*., 1985). The Hsp40 family is structurally diverse and members function to stimulate the Hsp70 ATP hydrolytic cycle (Liberek *et al*., 1991; Cyr *et al*., 1992) and some have the capacity to function as molecular chaperones (Wickner *et al*., 1991; Langer *et al*., 1992; Lu and Cyr, 1998a). Hsp40 proteins also act as specificity factors which direct Hsp70 to catalyze specific reactions in cellular protein metabolism (Silver and Way, 1993).

Hsp40 proteins with the potential to help Hsp70 facilitate CFTR biogenesis are Human DnaJ-1 (Hdj-1) and Hdj-2. Hdj-1 interacts with Hsp70 to fold nascent polypeptides as they emerge from cytosolic ribosomes and helps protect cells from thermal stress (Ohtsuka, 1993; Frydman *et al*., 1994; Terada *et al*., 1997). Hdj-2 contains a CaaX box (C, cysteine; a, any aliphatic amino acid; X, a polar amino acid) on its C-terminus (Chellaiah *et al*., 1993) and is predicted to be modified with isoprenoids (Zhang and Casey, 1996). A portion of farnesylated Hsp40 proteins are typically localized to the cytosolic surface of the ER (Caplan *et al*., 1993). If Hdj-2 is localized to the ER, this would position it to direct cytosolic Hsp70 to facilitate the folding of CFTRs cytosolic sub-domains just as they emerge from membrane tethered ribosomes.

We report that Hdj-2 is indeed localized to the cytoplasmic face of the ER and that it interacts with Heat shock cognate 70 (Hsc70) to suppress the aggregation of NBD1 on CFTR. Co-translational binding of Hdj-2/Hsc70 to NBD1 appears to stabilize it in an assembly-competent conformation and thereby promote protein assembly events which enable CFTR to reach its native state. One such assembly event appears to be the formation of intramolecular contacts between surfaces of NBD1 and the R-domain. These data suggest that Hdj-2/Hsc70 is an Hsp40/Hsp70 chaperone pair which can function to facilitate the biogenesis of membrane proteins that have large cytoplasmic domains.

Results

Hdj-2 co-localizes with ER markers

The localization of Hsp40 co-chaperone proteins plays a critical role in determining their ability to specify Hsp70 action in cellular protein metabolism (Brodsky *et al*., 1993; Ungermann *et al*., 1994; Cyr and Neupert, 1996). To determine whether Hdj-1 or Hdj-2 was more likely to function with Hsc70 to facilitate CFTR biogenesis, the localization of these Hsp40 proteins in cultured cells was compared by indirect immunofluorescence and digital confocal microscopy (Figure 1A and B). In 0.5 μm confocal sections of cells, Hdj-2 antibodies stained the cytosol and a perinuclear compartment. Perinuclear Hdj-2 staining overlapped extensively with the pattern of the ER marker calnexin (Figure 1B). On the other hand, Hdj-1 exhibited a diffuse cytoplasmic staining pattern that exhibited little overlap with calnexin. A portion of Hdj-2 is therefore localized to the ER, while another pool appears to be soluble. Hdj-1, on the other hand, does not appear to exhibit a specific staining pattern. In related studies we determined that Hdj-2, but not Hdj-1, is modified post-translationally with the isoprenoid farnesyl (data not shown). The partial localization of Hdj-2 to the ER surface is consistent with the localization observed for other farnesylated Hsp40 proteins (Caplan *et al*., 1992). Hdj-2 is positioned within the cell to promote reactions in protein metabolism that occur on the ER membrane surface.

Cytosolic Hsp70 and Hsp40 proteins can be co-immunoprecipitated with newly synthesized proteins

To examine the role of Hsc70 and its co-chaperones in CFTR biogenesis, we established experimental conditions to immunoprecipitate these and other cytosolic chaperones from cell extracts (Figure 2). Hsc70, Hdj-1, Hdj-2 and Tcp-1, a subunit of the cytosolic chaperonin Tric (Frydman *et al*., 1994), have all been shown to participate in cellular protein folding (Hartl, 1996). Antibodies to each of these proteins were acquired from commercial sources (see Materials and methods). When the antibodies against Hsc70, Hdj-1, Hdj-2 and Tcp-1 were utilized to probe Western blots of HeLa cell extracts they cross-reacted with only a single band which migrates on SDS–PAGE gels with the proper apparent molecular weight (Figure 2A, lanes 1, 4, 7 and 10). When HeLa cell extracts were incubated with the appropriate quantity of respective chaperone antibody (see Materials and methods for details) and protein G–agarose beads (PG), $<$80, 100 and 85% of Hsc70, Hdj-1 and Hdj-2 could be immunodepleted. In the case of Tcp-1, we could only deplete ~50% of it from cell lysates. When lysates were treated with PG alone little chaperone was removed and this suggested that the immunodepletion observed resulted from specific recognition of chaperone proteins by the respective antibodies against them.

In experiments where HeLa cells were metabolically labeled and then lysed with the non-ionic detergent Triton X-100, radiolabeled Hsc70, Hdj-1, Hdj-2 and Tcp-1 could be immunoprecipitated from cell extracts (Figure 2B).

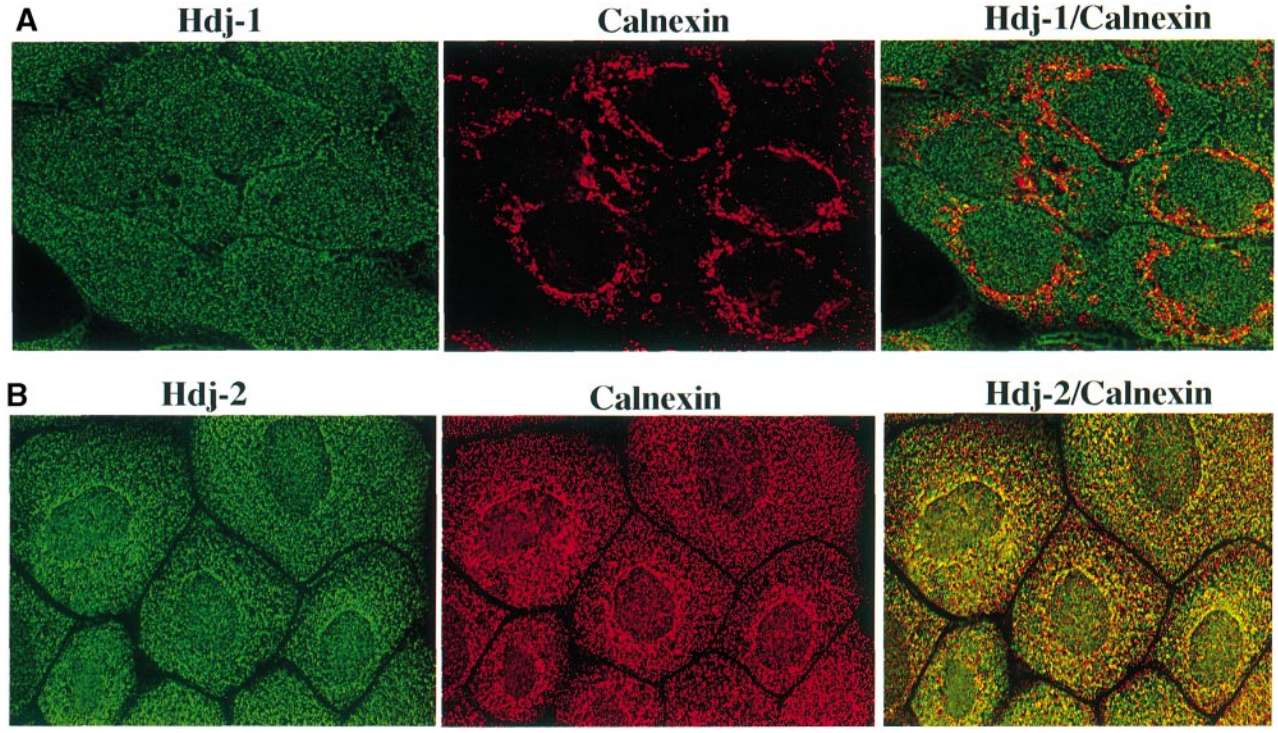

Fig. 1. Hdj-2 co-localizes with ER markers. (**A**) Decoration of CFPAC cells with rabbit polyclonal Hdj-1 and mouse monoclonal calnexin antibodies. (**B**) Decoration of CFPAC cells with mouse monoclonal Hdj-2 and rabbit polyclonal calnexin antibodies. To visualize the staining patterns of indicated primary antibodies, respective coverslips were decorated with goat anti-rabbit IgG–Oregon Green and goat anti-mouse IgG–Texas Red secondary antibodies. The localization of respective chaperone proteins was then determined in 0.5 μM optical sections of cells by digital confocal microscopy (see Materials and methods for details).

The relative intensity of the immunoprecipitated bands suggested that Hdj-2 was ~5-fold more abundant than Hdj-1, but present at concentrations that were similar to Hsc70. In Western blots, in which purified proteins were utilized as standards, Hsc70, Hdj-1, and Hdj-2 were found to represent 1.3, 0.05 and 0.23%, respectively, of total cell protein (Terada *et al*., 1997; data not shown). Purified Tcp-1 was not available to us, but literature results indicate that Tcp-1 is present in the cell at approximately one-third the level of Hsc70 (Frydman *et al*., 1994). Thus, the relative quantities of radiolabeled Hsc70, Hdj-1, Hdj-2 and Tcp-1 which we immunoprecipitated appear to accurately reflect the levels of these proteins in the cell.

A broad smear of newly synthesized protein could be co-immunoprecipitated with Hsc70, Hdj-1, Hdj-2 and Tcp-1 (Figure 2B). The quantity of newly synthesized protein that co-precipitated was proportional to the level of individual chaperones and significantly above the level of non-specific precipitation observed with non-immune IgG (Figure 2B, compare lane 2 with lanes 3–6). These data demonstrate our ability to immunoprecipitate Hsc70, Hdj-1, Hdj-2 and Tcp-1 from cell lysates. In addition, these data also demonstrate that, under native buffer conditions, we are able to isolate by co-immunoprecipitation, the complexes formed between molecular chaperones and newly synthesized polypeptides.

Hsc70 and Hdj-2 form complexes with CFTR and ΔF508 CFTR

To examine interactions between cytosolic chaperones and biogenic intermediates of CFTR and ΔF508 CFTR these proteins were transiently expressed in HeLa cells (see Materials and methods). Cells were then metabolically labeled and the processing of CFTR was monitored as an indicator of its progression through the secretory pathway (Denning *et al*., 1992; Ward and Kopito, 1994). On SDS–PAGE gels, the immature ER localized biogenic intermediate of CFTR, termed the B-form, migrates with a greater mobility than the maturely glycosylated C-form which has been transported out of the ER (Ward and Kopito, 1994). Immediately after the initial labeling period, we could detect CFTR and ΔF508 CFTR in the B-form (Figure 3A and B, lane 1) and during the 180 min chase period a significant portion of CFTR was converted to the C-form (Figure 3A, lane 7). ΔF508 CFTR is unable to exit the ER (Denning *et al*., 1992) and therefore we did not observe conversion of its B-form to C-form (Figure 3B, compare lane 1 with 7). These data establish that the CFTR and ΔF508 CFTR we express in HeLa cells represent biogenic intermediates which behave in a manner similar to forms of these proteins that are naturally expressed in epithelial cells.

When CFTR–chaperone complexes were analyzed, a band that migrated with a mobility that was identical to that of immature CFTR, but not mature CFTR, could be co-immunoprecipitated with Hsc70, Hdj-1, Hdj-2 and Tcp-1 (Figure 3A). At $T = 0$, on average ($n = 4$), the quantity of CFTR which could be co-precipitated with Hsc70, Hdj-1, Hdj-2, and Tcp-1 represented 19, 6, 9 and 2% of total CFTR, respectively. The amount of CFTR that could be co-immunoprecipitated with Hsc70, Hdj-1 and Hdj-2 was several fold above that isolated by non-specific immunoprecipitation with non-immune IgG (Figure 3A, compare lane 2 with lanes 3, 4 and 5). However, levels of CFTR

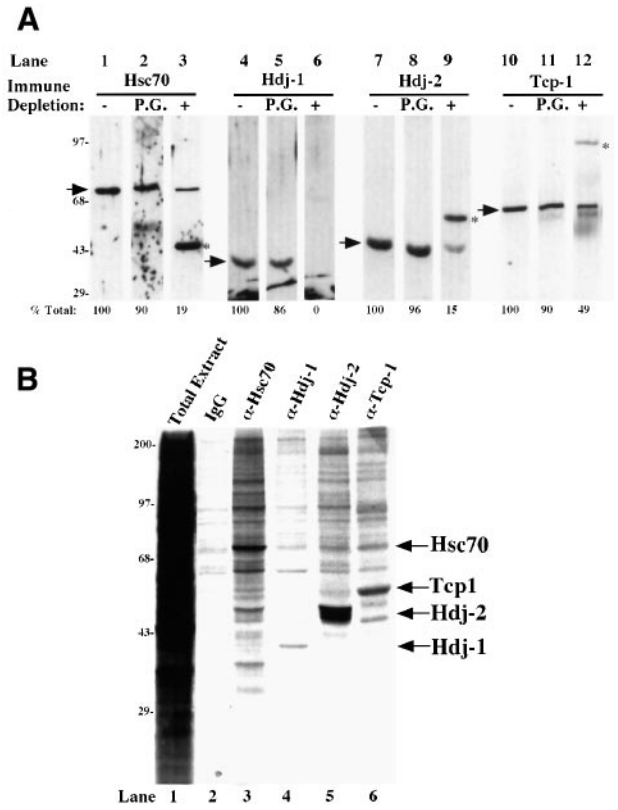

Fig. 2. Hsc70, Hdj-1, Hdj-2 and Tcp-1 form complexes with newly synthesized proteins. (**A**) Western blot analysis of HeLa cell extracts before and after immunodepletion of Hsc70, Hdj-1, Hdj-2 and Tcp-1. Immunodepletions were carried out as described below for the immunoprecipitation of chaperone proteins from metabolically labeled cell extracts. The symbols (+) and (–) indicate whether or not cell lysates were incubated with the indicated antibody and PG to immunodeplete the chaperone of interest. PG denotes lysates that were treated with only protein G–agarose beads. Numbers at the bottom of the gel in (A) denote quantitation of the signal generated from the respective chaperone proteins on each Western blot. Numbers are normalized to the total signal from lysates to which no antibody or protein G–agarose was added. The * band in lane 3 represents rat IgG that remains in cell extracts after their treatment with PG and is detected by sheep anti-rat IgG-HRP. The * band in lane 9 represents mouse IgG that remains in cell extracts after their treatment with PG and is recognized by goat anti-mouse IgG–HRP. The * band in lane 12 represents rabbit IgG that remains in cell extracts after their treatment with PG and is recognized by goat anti-rabbit IgG–HRP. (**B**) Immunoprecipitation of cytosolic chaperones from HeLa cell extracts. HeLa cells were metabolically labeled for 20 min with Tran^{35}S -label (100 μCi/1×10^6 cells). Cells were then lysed at 4°C under non-denaturing conditions in a buffer containing Mg-ATP and an ATP regenerating system as detailed in the Materials and methods section. Lysates were precleared with Pansorbin (2.0%) and antisera specific for Hsc70 (12.5 μg), Hdj-1 (0.5 μg), Hdj-2 (5.0 μg), Tcp-1 (2.5 μg) or mouse IgG (2.5 μg) was added to cell extracts (12.5 μg of total protein). Products of co-immunoprecipitation reactions were analyzed by SDS–PAGE and fluorography. IgG refers to non-immune mouse IgG that was utilized as a control to measure the level of labeled proteins that precipitate non-specifically. In the lanes labeled 'Total Extract' 10% of the labeled material used for co-immunoprecipitation reactions was loaded onto the gel. The mobility of molecular mass markers (in kDa) is indicated on the left of the gels.

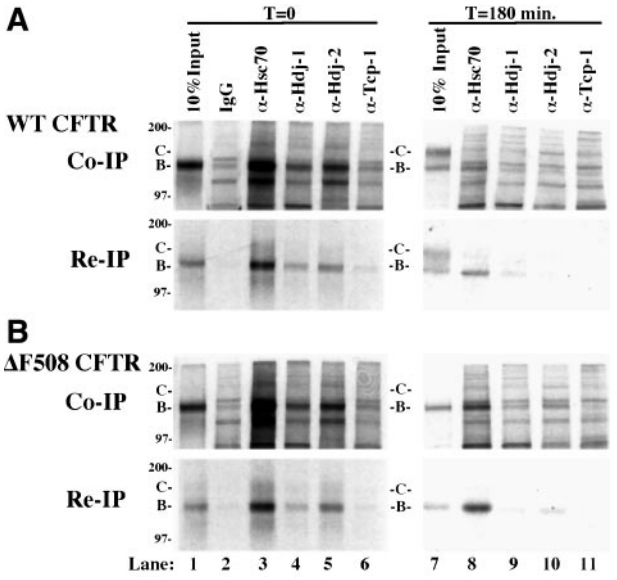

Fig. 3. Hsc70, Hdj-1 and Hdj-2 form complexes with immaturely glycosylated CFTR. HeLa cells were infected with vaccinia virus expressing T_7 RNA polymerase (vTF7-3) and transiently transfected with (**A**) pCDNA-CFTR or (**B**) pCDNA-ΔF508 CFTR. After an 8 h incubation, cells were metabolically labeled for 45 min with Tran^{35}S-label (100 μCi/1×10^6 cells). Cells were then analyzed for chaperone–CFTR complexes immediately (lanes 1–6) or incubated for an additional 180 min in DMEM + 10% FBS (lanes 8–12). The sample in lane 1 was prepared by immunoprecipitating CFTR with α-CFTR under denaturing conditions and 10% of the total protein isolated by this method was run on the gel. To isolate chaperone CFTR complexes, cell lysates were made under non-denaturing conditions, precleared with Pansorbin and antisera to the indicated chaperone proteins was added. Immune complexes were then precipitated with PG. To definitively identify CFTR in co-precipitates products of the co-immunoprecipitation reactions were split. One portion was immediately run on SDS–PAGE gels and the results from this analysis are shown in the panel denoted as Co-IP. The other portion was subjected to a second round of immunoprecipitation under denaturing conditions with α-CFTR under denaturing conditions and the results of this analysis are exhibited in the panels denoted as Re-IP. In an attempt to normalize the signals for these different experimental protocols, gels from the Re-IP experiments were exposed to X-ray film for twice as long as the Co-IPs. IgG indicates non-immune mouse IgG used as a control for co-immunoprecipitations. 'B' marks the mobility of the ER-localized, core-glycosylated, immature form of CFTR. 'C' denotes the position on gels of the complex-glycosylated, mature form of CFTR. Numbers on the left of each panel indicate the migration of molecular mass markers (in kDa).

that co-precipitated with Tcp-1 were very to close to the level of background precipitation (Figure 3A, compare lanes 2 and 6).

A complication to the interpretation of results from the co-immunoprecipitation experiments presented in Figure 3, was the observation that a number of radio-labeled bands in addition to the putative B-form of CFTR were also co-precipitated with chaperone proteins. These data raised the possibility that the band on gels which migrated with the same mobility as CFTR might be of some other origin. To rule out this possibility we demonstrated that the band designated as the B-form of CFTR in co-immunoprecipitates could be re-immunoprecipitated in a second reaction, under denaturing conditions, with α-CFTR sera (Figure 3A, Re-IP).

A number of observations suggest that the CFTR–chaperone complexes isolated represent specific intermediates of the CFTR biogenic pathway. Firstly, the quantity of CFTR that was co-precipitated with Hsc70, Hdj-1 and Hdj-2 was routinely several times greater than the amount that was non-specifically precipitated with non-immune IgG (compare Figure 3A, lane 2 with lanes 3, 4 and 5). The total level of the CFTR–chaperone complexes formed in the cell may be underestimated in

these experiments because chaperone–substrate complexes tend to dissociate during isolation (Ungermann *et al*., 1994, 1996). Secondly, the binding of CFTR appeared to be specific for the chaperone protein in question. CFTR formed much higher levels of complex with Hsp70 and Hsp40 proteins than with Tcp-1 (Figure 3). In contrast, Tcp-1 could co-precipitate quantities of newly synthesized protein that were similar to Hsc70 and Hdj-2 (Figure 2). Finally, the ability of Hsp70 and Hsp40 proteins to bind CFTR appeared to be dependent upon its conformation. Hsc70, Hdj-1 and Hdj-2 were observed to bind immature, but not mature forms, of CFTR (Figure 3A, compare $T = 0$ with $T = 180$).

ΔF508 CFTR exhibits subtle defects in its folding pathway that cause assembly intermediates to accumulate and limit its ability to reach the native state (Qu *et al*., 1997; Zhang *et al*., 1998). To determine whether Hsp70 and Hsp40 proteins bind CFTR and ΔF508 CFTR differentially, we examined their interactions with chaperones. When interactions between ΔF508 CFTR and Hsc70, Hdj-1, Hdj-2 and Tcp-1 were examined at $T = 0$ and then compared with results obtained with CFTR, the levels of ΔF508 CFTR–Hsc70 and ΔF508 CFTR–Hdj-2 complexes were 1.9±0.2-fold and 1.6±0.1-fold ($n = 5$) more abundant than similar complexes with CFTR. However, levels of complex formed between ΔF508 CFTR and Hdj-1 and Tcp-1 appeared unchanged. To obtain these data we quantitated the amount of CFTR and ΔF508 CFTR that could be co-immunoprecipitated with chaperone proteins and then normalized these values to the total amount of CFTR and ΔF508 CFTR which was immunoprecipitated directly with α-CFTR (Figure 3A and B).

Next, we compared the half-life of CFTR–chaperone and ΔF508 CFTR–chaperone complexes (Figure 4). Since complexes between Hsc70 and Hdj-2 appeared most sensitive to the ΔF508 mutation (Figure 3B), in this set of experiments, only complexes between these chaperones and CFTR were examined. CFTR and ΔF508 CFTR were expressed at similar levels and over the time course of the 90 min chase period, the signal for the immature form of each decayed in a time-dependent manner (Figure 4A). At the beginning of the chase period complexes between ΔF508 CFTR and Hsc70 and Hdj-2 were ~2-fold more abundant than those with CFTR (Figure 4B and C, compare lanes 1 and 5). Throughout the time course of the chase period, ΔF508 CFTR–chaperone complexes became progressively more abundant than similar complexes with CFTR. Collectively these data suggest that Hsc70 and Hdj-2 exhibit differences in their ability to interact with wild-type and mutant forms of CFTR.

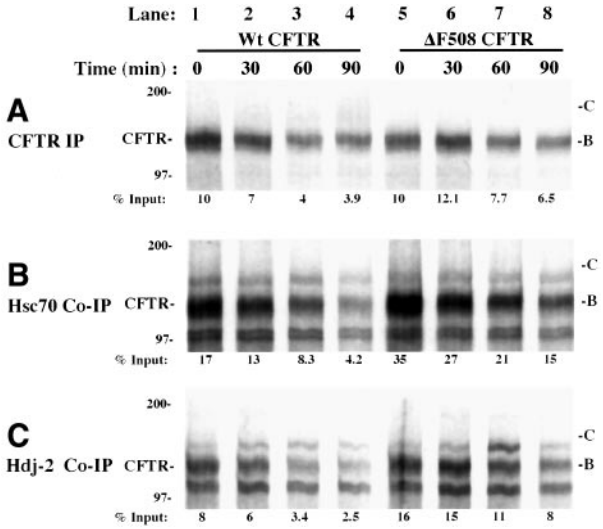

Fig. 4. Complex formation between ΔF508 CFTR and Hsc70 and Hdj-2 is greater than that with CFTR. HeLa cells were infected with vaccinia virus (vTF7-3) and transiently transfected with pCDNA-CFTR or pCDNA-ΔF508 CFTR. After an 8 h incubation, cells were metabolically labeled for 15 min with Tran^{35}S-label (100 μCi/1×10^6 cells). Complex formation between the respective proteins and molecular chaperones were then analyzed by co-immunoprecipitation as described in the legend to Figure 3. Cell lysates were produced at the indicated time points and were precleared with Pansorbin. In (**A**), α-CFTR was added to cell lysates and immunoprecipitations were carried out under denaturing conditions. Ten percent of the material isolated in the immunoprecipitation reaction carried out at the respective time points was then loaded on SDS–PAGE gels and analyzed. Quantitation of gels was then performed by densitometric analysis and values shown in lanes 2–4 are normalized to the signal for immature CFTR at $T = 0$ in lane 1. In (**B**) and (**C**), antisera against Hsc70 and Hdj-2, respectively, was added to cell lysates and co-immunoprecipitations were carried out under non-denaturing conditions (see Materials and methods for details). Quantitation of immature CFTR and ΔF508 CFTR which could be co-immunoprecipitated with Hsc70 or Hdj-2 was performed by densitometric analysis and the values shown are expressed as % of the total CFTR and ΔF508 CFTR that could be isolated by immunoprecipitation at $T = 0$ and shown in (A). 'B' denotes the ER localized, core-glycosylated, immature form of CFTR. 'C' denotes the complex-glycosylated, mature form of CFTR. Numbers on the left of each panel denote the mobility of molecular mass markers in kDa.

Hdj-2 and Hsc70 bind truncated fragments of CFTR in a domain-specific manner

What aspects of CFTR biogenesis do Hsc70 and Hdj-2 facilitate and to what regions of the protein do they bind? To address these questions, the stage of biosynthesis at which Hsc70 and Hdj-2 first interact with CFTR was investigated. This was accomplished by determining the ability of these chaperones to form complexes with different length CFTR fragments which resemble authentic biogenic intermediates (Sheppard *et al*., 1994; Ostedgaard *et al*., 1997; Lu *et al*., 1998). Respective fragments examined contain stop codons after MSD1 (CFTR 370X), NBD1 (CFTR 593X), the R-domain (CFTR 837X), and MSD2 (CFTR 1162X). CFTR 837X is similar to a differentially spliced form of CFTR which is naturally expressed in the developing kidney (Devuyst *et al*., 1996). CFTR 1162X is a form of CFTR identified in a family that is afflicted with cystic fibrosis (Gasparini *et al*., 1992). The clinical symptoms exhibited by patients that harbor CFTR 1162X are considered mild, which suggests that a portion of this protein is capable of folding and functioning as an ion channel (Gasparini *et al*., 1992).

Before we analyzed complex formation between these CFTR fragments and chaperone proteins, their expression in HeLa cells was characterized to determine the optimal conditions for this analysis. Cells were transfected with increasing concentrations of the respective CFTR expression plasmids and the synthesis of each fragment was monitored by immunoprecipitation (Figure 5A). The expression of each CFTR fragment was found to occur in a dose-dependent manner with synthesis leveling off somewhere between 0.5 and 2.5 μg of DNA/culture well.

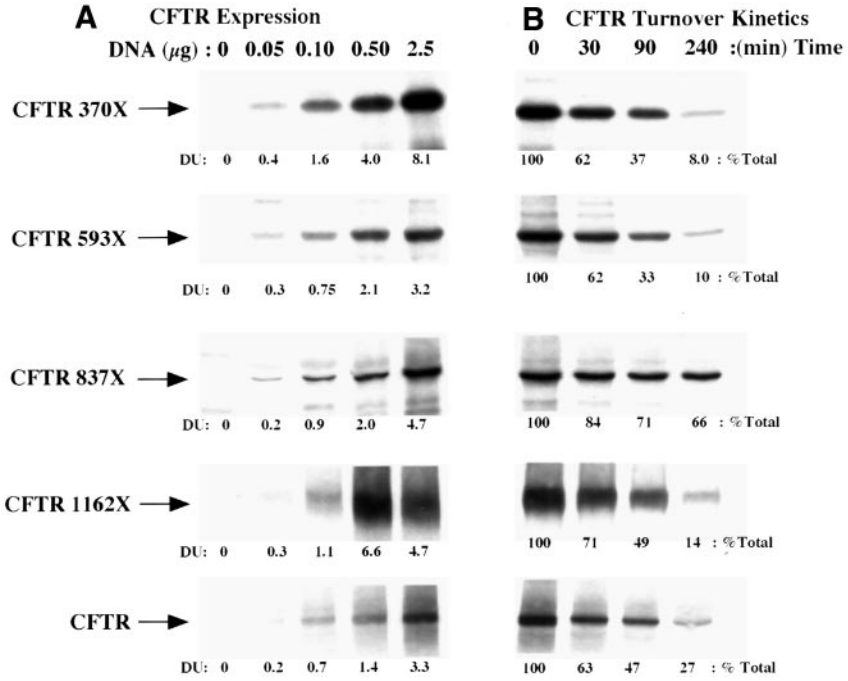

Fig. 5. Examination of expression and turnover kinetics of CFTR fragments in HeLa cells. (**A**) Dependence of CFTR expression on the concentration of DNA transfected into HeLa cells. Cells were infected with vaccinia virus (vTF7-3) and transiently transfected with the indicated amounts of DNA encoding CFTR fragments or full-length CFTR as indicated. After an 8 h incubation, cells were metabolically labeled for 15 min. with Tran^{35}S-label (100 μCi/1×10^6 cells) and lysed under denaturing conditions. Lysates were then precleared with Pansorbin and the respective CFTR fragments were immunoprecipitated with anti-sera against the N-terminal region which is common to each. In control experiments, we found that >90% of each respective fragment could be isolated in the detergent soluble fraction of cells and therefore did not behave like a protein that had aggregated (data not shown; Ward and Kopito, 1994). (**B**) Examination of CFTR turnover kinetics. Cells were infected with vaccinia virus (vTF7-3) and transiently transfected with 0.25 μg of DNA encoding CFTR fragments or CFTR as indicated. After an 8 h incubation, cells were metabolically labeled as described above. Cell lysates were made immediately or following a period. After lysis, CFTR or CFTR fragments were immunoprecipitated and analyzed by SDS–PAGE and fluorography. For (A) the quantitation of the expression level of respective CFTR fragments is exhibited in arbitrary densitometric units (DU). In (B), values from quantitation of the different CFTR fragments are expressed as a % of the total CFTR fragment present at $T = 0$.

All the CFTR fragments were expressed at a similar level and we therefore chose to transfect cells with 0.25 μg of the respective expression plasmids to ensure that the synthesis of each was at the low end of the linear range. Under these experimental conditions, CFTR and its fragments represent ~0.5–1% of total cell protein and are therefore are not grossly overexpressed (data not shown). We have also determined that >90% of each respective CFTR fragment expressed in HeLa cells partitions in the detergent soluble fraction of extracts and therefore are not prone to aggregation (data not shown).

When the turnover kinetics of the respective fragments was examined, CFTR 370X, CFTR 593X, CFTR 1162X and CFTR all had a half-life of 30–90 min (Figure 5B). Strikingly, CFTR 837X had a half-life that was ~8 times longer than that of CFTR and the other fragments we expressed. In related studies, the Skatch group has examined the half-life of CFTR 836X expressed in oocytes and found that 80% of this protein was capable of folding to a conformation that enables it to persist in cells for 24 h, whereas shorter CFTR fragments are completely degraded during this time period (Xiong *et al*., 1997). Together, these data suggest that sub-domains within the first 836 amino acid residues of CFTR are capable of folding to a conformation that is more resistant to proteolytic digestion than other forms of CFTR, including the full-length protein.

Next, we examined the ability of Hsc70 and Hsp40 proteins to bind these different length CFTR fragments (Figure 6). This analysis was carried out by determining which if any of the different length CFTR fragments could be co-immunoprecipitated with Hsc70, Hdj-1 and Hdj-2 (Figure 6A). Figure 6, lane 1, shows 10% of the quantity of the respective CFTR that was isolated by direct immunoprecipitation under denaturing conditions with α-CFTR. Lane 2 shows the profile of radiolabeled proteins which were non-specifically isolated with non-immune IgG under native buffer conditions. For all of the CFTR fragments tested, non-specific immunoprecipitation represented <0.7% of total input. The amount of CFTR isolated in complexes with chaperone proteins was 3- to 28-fold greater than the quantity of non-specific immunoprecipitation observed. To identify definitively the CFTR fragments that were isolated in the co-precipitates shown in Figure 6A, the products of native immunoprecipitation reactions were re-immunoprecipitated under denaturing conditions with α-CFTR (Figure 6B). Of the many radiolabeled bands present in co-precipitates, the only band that could be re-immunoprecipitated with α-CFTR was the one that migrated with the same mobility as the CFTR fragment in Figure 6B, lane 1. These data indicate that we are able to co-immunoprecipitate specific complexes between different CFTR fragments and cytosolic Hsp70 and Hsp40 chaperone proteins.

From the comparison of the levels of complex formation between chaperone proteins and different length CFTR

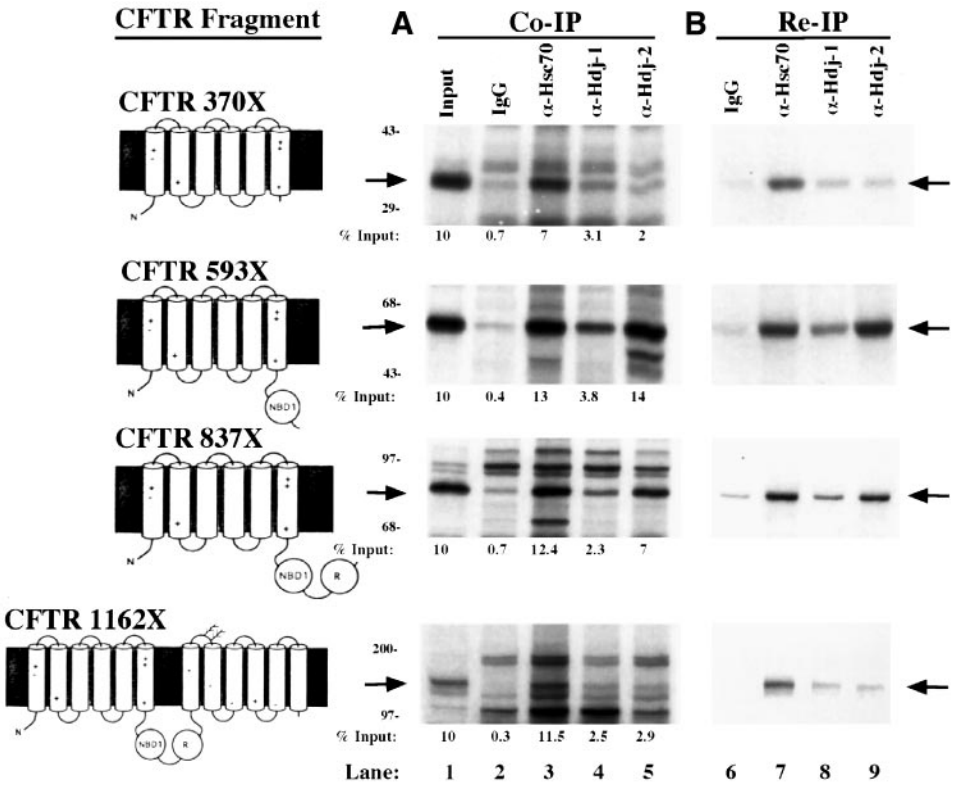

Fig. 6. Hsc70 and Hdj-2 form complexes with CFTR fragments in a domain-specific manner. HeLa cells were infected with vaccinia virus (vTF7-3) and transiently transfected with the CFTR fragments indicated on the left of the respective panels. After an 8 h incubation, cells were metabolically labeled for 15 min with Tran^{35}S-label (100 μCi/1×10^6 cells) and lysed under non-denaturing conditions. Cell lysates were then precleared, antisera was added as indicated and co-immunoprecipitations and re-immunoprecipitations were carried out as described in the legend to Figure 3. (**A**) and (**B**) exhibit the results from co-immunoprecipitation and re-immunoprecipitation reactions, respectively. Input represents 10% of the total CFTR which could be directly immunoprecipitated from cell extracts under denaturing conditions with α-CFTR. Quantitation of CFTR fragments that could be co-immunoprecipitated with IgG, Hsc70, Hdj-1 or Hdj-2 was performed by densitometric analysis and the values shown are normalized to the input for each respective fragment. The schematics represent models for the domain structures of the respective CFTR fragments. Numbers shown on the left of panels denote the migration of molecular mass markers in kDa.

fragments we report a number of novel findings. CFTR 370X could be co-immunoprecipitated with Hsc70, but levels of complex formation between it and Hdj-1 and Hdj-2 were relatively low (Figure 6A). However, upon expression of NBD1 on CFTR 593X there was a dramatic 7-fold increase in the ability of Hdj-2, but not Hdj-1 to bind CFTR. Compared with CFTR 370X, there was also a nearly 2-fold increase in the level of complex formation between Hsc70 and CFTR 593X. Expression of the R-domain on CFTR 837X, lead to a 50% decrease in the quantity of CFTR fragment which could be isolated in a complex with Hdj-2, but complex formation with Hsc70 was not markedly reduced. Expression of MSDII on CFTR 1162X further reduced the quantity of CFTR fragment that could be co-immunoprecipitated with Hdj-2, but levels of complex formation with Hsc70 and Hdj-1 remained similar to those observed with CFTR 837X.

These data suggest that a region within the first 370 residues of CFTR can be bound stably by Hsp70. Yet upon the expression of NBD1 in the cytosol, additional binding sites for Hsc70 appear to be exposed and now Hdj-2 can also recognize CFTR. After expression of the R-domain, a portion of CFTR appears to assemble into a conformation in which some of the binding sites for Hdj-2 are no longer exposed. Then after expression of MSDII on CFTR 1162X, binding sites for Hdj-2 are almost completely buried, while an apparently different set of binding sites for Hsc70 remain exposed. Thus, Hdj-2 and Hsc70 bind CFTR fragments in a transient and domain-specific manner. Hdj-1 can also bind to CFTR fragments, but its interactions are not dynamic and therefore more difficult to interpret. Since the binding of Hdj-2 to CFTR fragments is dramatically increased by expression of the NBD1, and decreased by expression of the R-domain and MSDII, the Hdj-2/Hsc70 chaperone pair may facilitate the co-translational assembly of NBD1 into an intramolecular complex with regions within the C-terminal half of CFTR.

Hdj-1, Hdj-2 and Hsp70 can bind ribosome-bound CFTR translation intermediates

If Hsc70 and Hdj-2 promote the co-translational assembly of CFTR, they should be able to gain access to translation intermediates while they are associated with the ribosomes. To address this issue, membrane-inserted and ribosome-bound CFTR translation intermediates were generated and their ability to interact with cytosolic chaperones was examined. This was accomplished by programming reticulocyte lysates with truncated mRNAs which lack a stop codon and supplementing the lysates with canine pancreas microsomes (Perara *et al*., 1986). The CFTR translation intermediates synthesized via this method were CFTR 430, CFTR 776 and CFTR 897. To monitor insertion of these translation intermediates into microsomal membranes, the glycosylation site normally present in

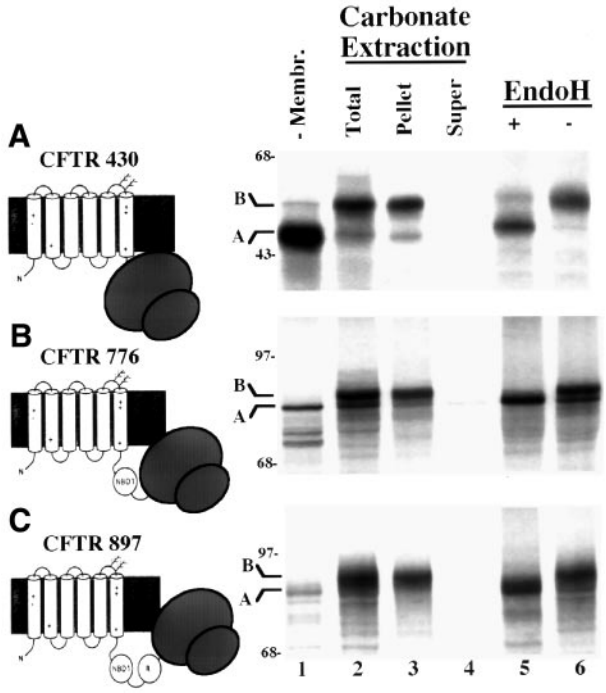

Fig. 7. Characterization of CFTR that was translated *in vitro*. *In vitro* translation of (**A**) CFTR 430, (**B**) CFTR 776 or (**C**) CFTR 897 was carried out as described in the Materials and methods section. All *in vitro* translations of CFTR were carried out in a 100 μl reaction volume for 60 min at 30°C. All reactions contained canine microsomal membranes except those in lane 1. At the end of the incubation period, 20 μg/ml cycloheximide was added to inhibit additional protein synthesis and reactions were placed on ice. Aliquots (10 μl) were then removed and subjected to post-translational analysis. One aliquot did not receive further treatment (lane 2). Another aliquot was incubated for 30 min at 0°C with 100 mM sodium carbonate pH 11.0. This sample was then centrifuged through a 0.5 M sucrose cushion and separated into pellet (lane 3) and supernatant (lane 4) fractions. Two other aliquots were solubilized with 0.1% Triton X-100 and one was treated with 0.25 units of Endo H and incubated for 2 h at 30°C (lane 5) and the other was mock-treated (lane 6). Proteins in the respective samples were then solubilized with SDS–sample buffer and analyzed by SDS–PAGE. 'A' and 'B' denote, respectively, the non-glycosylated and core glycosylated forms of CFTR. Schematics shown represent models of the respective CFTR fragments that were translated in reticulocyte lysates. The mobility of molecular mass markers (in kDa) on SDS–PAGE gels is indicated on the left.

extracellular loop 4 was inserted between transmembrane domains 5 and 6. CFTR that contains a glycosylation site in this position is processed normally and does not appear to misfold (Chang *et al*., 1994). When CFTR 430, 776 and 897 were translated in the absence of microsomes, products ran on SDS–PAGE gels as a single band (Figure 7). In the presence of microsomes the migration of these CFTR translation intermediates was retarded in a manner consistent with their glycosylation in the ER. Indeed, treatment of these three different translation intermediates with endoglycosidase H (EndoH) increased the mobility of translation products to those observed in the absence of microsomes. The glycosylated form of each respective translation product also appeared to be properly inserted into microsomes since they could not be extracted from these membranes with sodium carbonate (Figure 7). These data indicate that CFTR 430, 776 and 897 represent membrane-inserted translation intermediates of CFTR.

In co-immunoprecipitation experiments (Figure 8), CFTR 430 could be co-immunoprecipitated with Hsc70 and Hdj-1, but not Hdj-2. CFTR 776 contains MSD1, NBD1 and is truncated in the middle of the R-domain. Compared with CFTR 430, a larger portion of CFTR 776 could be co-immunoprecipitated with Hsc70, Hdj-1 and Hdj-2. Apyrase treatment of lysates to reduce ATP levels resulted in a several fold increase in the quantity of CFTR 776 which was co-immunoprecipitated with Hsc70, but significantly reduced the levels of complexes with Hdj-2. On the other hand, ATP depletion did not alter our ability to co-immunoprecipitate Hdj-1 with CFTR 776. In experiments with CFTR 897 (Figure 8C), which contains the complete R-domain instead of the truncated version found in CFTR 776, there was a dramatic reduction in the relative level of complex formation with Hdj-2, but interactions with Hdj-1 and Hsc70 were not altered dramatically.

These data indicate that Hsc70 and Hdj-2 can bind translation intermediates of CFTR while they are associated with membrane-tethered ribosomes. As observed with CFTR fragments expressed in HeLa cells, binding of Hsc70 and Hdj-2 to CFTR was dependent upon the expression of NBD1 in the cytosol and was dynamic. Binding of Hsc70 and Hdj-2 to CFTR also appeared to be mechanistically distinct. Depletion of ATP from reticulocyte lysates enhanced complex formation with Hsc70 but nearly abolished Hdj-2 binding. The basis for this difference appears to be related to the fact that the ADP-form of Hsc70 binds substrates with higher affinity than ATP-form and that Hsp40 proteins function as molecular chaperones independent of this nucleotide (Cyr, 1997).

Hdj-2 and Hsc70 cooperate to suppress the aggregation of NBD1

Results from co-immunoprecipitation experiments suggest that Hsc70 and Hdj-2 cooperate to promote protein–protein interactions between NBD1 and other regions of CFTR by suppressing its aggregation until its assembly partners in the C-terminal portion of CFTR can be synthesized. To support this conclusion, we needed to demonstrate that (i) Hdj-2 can functionally interact with Hsc70 and (ii) Hdj-2 is capable of functioning as a molecular chaperone to suppress NBD1 aggregation.

Therefore we tested whether purified Hdj-2 was capable of interacting with Hsc70 to stimulate its ATPase activity and compared this action with that of Hdj-1 (Figure 9A). Hdj-2 and Hdj-1 both stimulated ADP formation by Hsc70 ~6-fold and this occurred in a dose-dependent manner. Maximal stimulation of ATP hydrolysis by both co-chaperones occurred at 1:1 Hsc70:Hsp40 molar ratios and the kinetics of ADP formation were linear for at least 20 min. These data demonstrate for the first time that Hdj-2 can regulate Hsc70 ATPase and indicates that it does so in a manner similar to Hdj-1 (Freeman *et al*., 1995; Minami *et al*., 1996).

To test whether Hdj-2 functions as a molecular chaperone to facilitate CFTR biogenesis, its ability to suppress the aggregation of NBD1 folding intermediates was compared with that of Hdj-1 (Figure 9B and C). When purified NBD1 was completely denatured and then diluted from denaturant into a folding buffer, to a final concentration of 0.5 μM, it was observed to aggregate

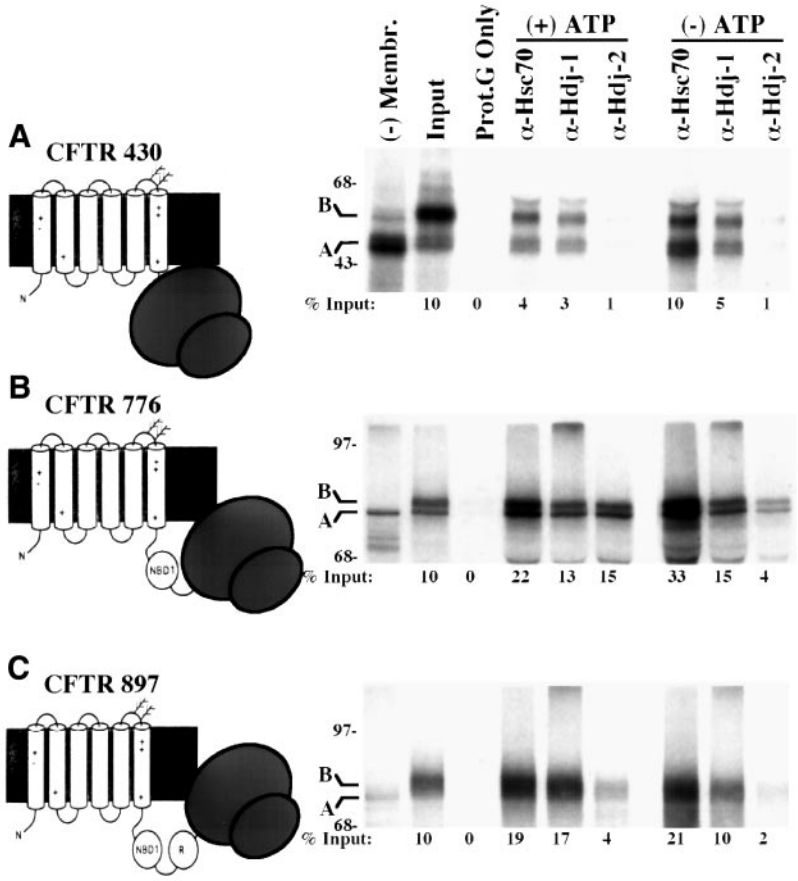

Fig. 8. Co-immunoprecipitation of *in vitro*-translated CFTR with Hsc70, Hdj-1 and Hdj-2. *In vitro* translation of (**A**) CFTR 430, (**B**) CFTR 776 or (**C**) CFTR 897 was performed as described in the Materials and methods. After translation for 60 min at 30°C, 20 μg/ml cycloheximide was added to inhibit additional protein synthesis. Reactions were then split into two aliquots with one being mock-treated and to the other, 0.25 units of apyrase/μl was added to reduce ATP levels. Complex formation between the respective CFTR translation products and cytosolic chaperones was then analyzed by determining their ability to be specifically co-immunoprecipitated with Hsp70, Hdj-1 and Hdj-2. 'A' and 'B' denote, respectively, the non-glycosylated and core glycosylated forms of CFTR translation products. Greater than 80% of translation products were typically in the 'B' form. In (A–C), 'input' represents 10% of the total CFTR that could be directly immunoprecipitated from translation reactions. Quantitation of translation intermediates which could be co-immunoprecipitated with chaperone proteins was performed by densitometric analysis and the values shown are normalized to the input. The schematics represent models of the respective CFTR fragments generated *in vitro*. The mobility of molecular mass markers (in kDa) is indicated on the left.

over time. Inclusion of Hdj-1 at ⩽10 μM had little detectable influence on the rate or extent of NBD1 aggregation (Figure 9B). In contrast, Hdj-2 functioned as a chaperone in a concentration-dependent manner to suppress NBD1 aggregation (Figure 9C). Maximal suppression of NBD1 aggregation was observed at a 5:1 Hdj-2:NBD1 molar ratio.

When tested in combination, Hdj-1 and Hdj-2 were both able to enhance the action of Hsc70 in suppressing NBD1 aggregation (Figure 9B and C). However, the Hdj-2/Hsc70 chaperone pair acted in superior fashion to Hdj-1/Hsc70. The combination of Hdj-1 and Hsc70 suppressed the rate of NBD1 aggregation by ~50%, whereas Hdj-2/Hsc70 could suppress >85% of this reaction. The ability of the different combinations of Hsp70 and Hsp40 chaperone pairs to suppress NBD1 aggregation was dependent upon the presence of ATP. This result suggests that these Hsp70 and Hsp40 proteins must interact in order to suppress NBD1 aggregation.

These data provide evidence that Hdj-2 can act alone and/or in combination with Hsc70 to suppress NBD1 aggregation. Additionally, these data provide evidence that the chaperone action of Hdj-1 is not equivalent to that of Hdj-2. This observation helps explain why we observe large differences in the ability of Hdj-1 and Hdj-2 to interact with CFTR biogenic intermediates.

Discussion

We have demonstrated that Hdj-2 and Hsc70 interact with early stage biogenic intermediates of CFTR in the ER. The interactions observed between CFTR translation intermediates and Hsc70 and Hdj-2 are deemed functionally relevant because they are transient, ATP-dependent and domain-specific. A function of the Hsc70/Hdj-2 pair appears to be the co-translational stabilization of NBD1 and the promotion of intramolecular assembly events between it and the R-domain. Numerous polytopic membrane proteins expose large sub-domains to the cytosol and our data suggest that Hdj-2 is capable of acting with Hsc70 to facilitate the folding/assembly of polypeptides in this class.

Interpretations of the data we present and those of others allow us to propose the following pathway for CFTR assembly. CFTR is 1480 amino acid residues in length and its translation occurs at a rate of 2.7 residues

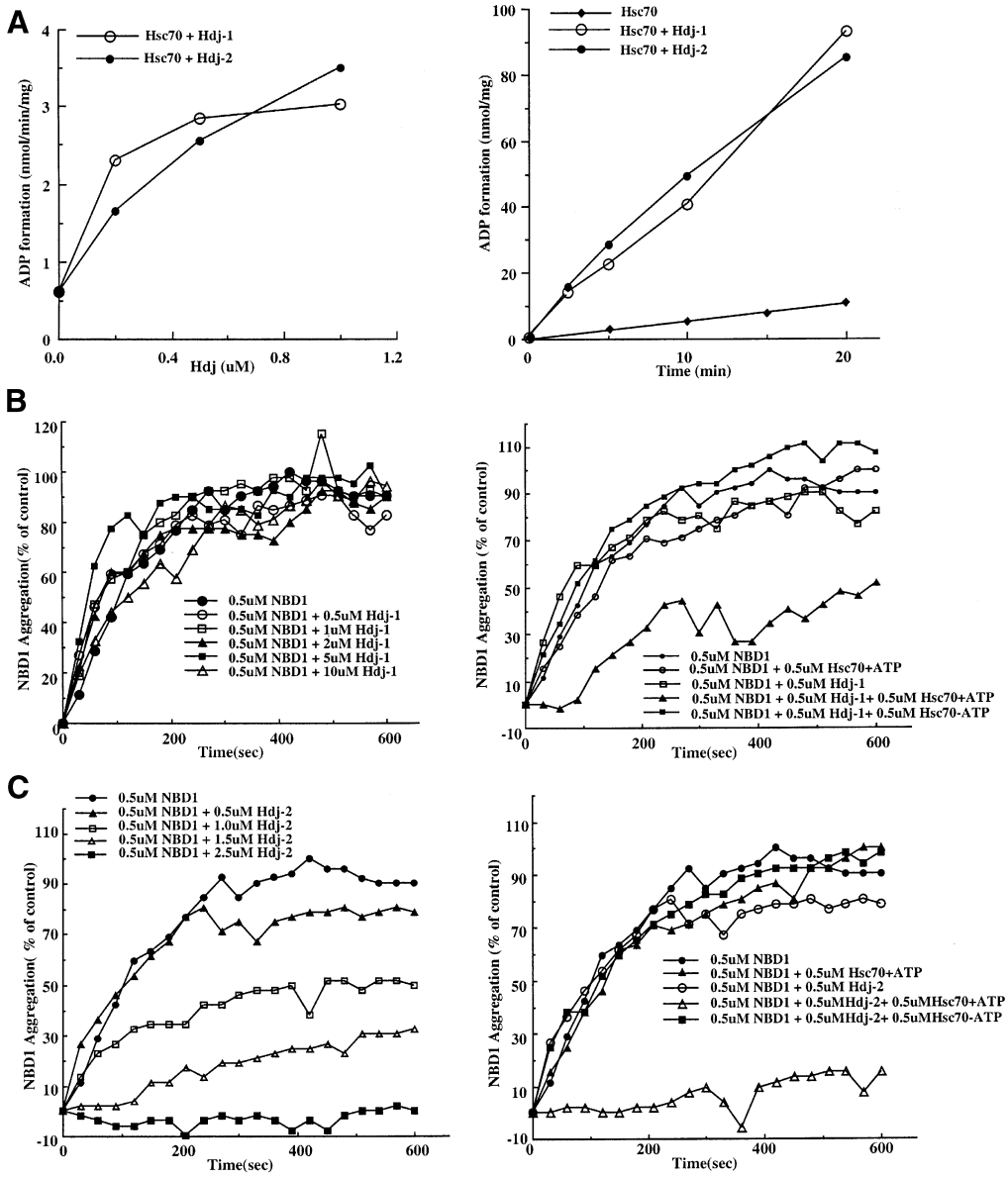

Fig. 9. Hdj-2 and Hsc70 cooperate to suppress the aggregation of NBD1 folding intermediates. (**A**) Hdj-1 and Hdj-2 stimulate the ATPase activity of Hsc70. In the left panel, Hsc70 (0.5 μM) was incubated with [α-^{32}P]ATP (50 μM; 2.0–3.0×10^5 c.p.m./pM) for 10 min at 30°C and Hdj-1 or Hdj-2 were added as indicated. In the right panel, the kinetics of Hsc70 (0.5 μM) ATPase activity in the presence of Hdj-1 (1 μM) and Hdj-2 (1 μM) were determined. Hdj-1 and Hdj-2 were not capable of hydrolyzing ATP independently of Hsp70 (data not shown). Data exhibited in the two panels represent the average of two independent experiments. (**B**) Suppression of NBD1 aggregation by Hdj-1 and Hsc70. Purified NBD1 was denatured with 6 M guanidinium–HCl and then diluted out of denaturant into folding buffer which was supplemented with Hdj-1 (left panel) or the combination of Hdj-1 and Hsc70 (right panel). (**C**) Reactions were carried out as in (B) except Hdj-2 was substituted for Hdj-1 in reactions. Aggregation of NBD1 was monitored by light scattering at 25°C in a spectrophotometer set at 320 nm.

per second, so it takes ~9 min to be synthesized (Ward and Kopito, 1994). Hence, the assembly of MSD1 (350 residues), NBD1 (185 residues), R-domain (245 residues), MSD2 (290 residues) and NBD2 (244 residues) into a native tertiary structure has ample time to initiate co-translationally (Fedorov and Baldwin, 1997). Insertion and orientation of transmembrane domains within MSD1 into the ER membrane represents the first step in CFTR folding (Lu *et al*., 1998). After NBD1 is synthesized and extruded into the cytosol it is bound transiently by Hdj-2 and then Hsc70. The Hdj-2/Hsc70 pair might then promote NBD1 folding (Strickland *et al*., 1997) or may simply stabilize it during the 90 s period estimated to be required for R-domain synthesis. The R-domain then interacts with the N-terminal half of CFTR in a manner that reduces Hdj-2 binding. Perhaps NBD1 and the R-domain form a complex which buries some of the binding sites on CFTR for Hdj-2. MSD2 is then synthesized, integrated into the ER membrane and this event appears to stabilize NBD1–R-domain interactions which leads to the release of most of the Hdj-2 from CFTR. The stabilization of NBD1–R-domain interactions may involve the formation of an MSD1–MSD2 complex within the ER membrane (Ostedgaard *et al*., 1997) and this is also a critical step in formation of the CFTR channel (Ostedgaard *et al*., 1997). Interactions between MSD1 and MSD2 might be facilitated

by the molecular chaperone calnexin (Pind *et al*., 1994). Finally, NBD2 is synthesized and conformational maturation of CFTR is completed in a process that requires ATP (Lukacs *et al*., 1994). Since Hsc70 and Hdj-2 are also found in association with full-length CFTR biogenic intermediates, the final maturation steps involving NBD2 might also involve the action of this cytosolic Hsp70/Hsp40 chaperone pair.

Evidence to support the inclusion of a step in the CFTR folding pathway in which Hdj-2 facilitates protein–protein interactions between NBD1 and the R-domain is as follows. First, we have demonstrated that Hdj-2 forms complexes with regions of CFTR translation intermediates that correspond to NBD1. Secondly, Hdj-2 functions with Hsc70 to suppress the aggregation-purified NBD1. Thirdly, upon synthesis of the R-domain, Hdj-2 is no longer observed to strongly interact with ribosome-bound CFTR translation intermediates. Finally, there is evidence to suggest that NBD1 and the R-domain interact during the normal regulation of CFTR function (Winter and Welsh, 1997). The R-domain modulates CFTR channel activity by altering the affinity of NBD1 for ATP (Winter and Welsh, 1997) and the mechanism behind this regulatory event might involve direct NBD1–R-domain interactions.

We observed that complexes between Hsc70 and Hdj-2 with immature ΔF508 CFTR were ~2-fold more abundant than similar complexes with CFTR. Therefore, ΔF508 CFTR appears to have more difficulty than CFTR in progressing to a point in its folding pathway where it buries binding sites for Hdj-2 and Hsc70. This is interpretation is consistent with the observation made by the Lukacs group that at early stages of assembly, immature CFTR and ΔF508 CFTR exist in similar conformations, but only the wild-type form can progress on its folding pathway to attain a native conformation (Zhang *et al*., 1998). An explanation for the assembly defect observed with ΔF508 CFTR, based on the data we present, is that ΔF508 NBD1 is unable to efficiently interact with the R-domain or other regions in the C-terminus. Such an assembly defect could cause chaperone-binding sites on CFTR to remain exposed and contribute to the diversion of ΔF508 CFTR from its biogenic pathway to the ubiquitin–proteasome pathway for degradation (Jensen *et al*., 1995; Ward and Kopito, 1995; Lukacs *et al*., 1994).

In comparing results obtained with CFTR fragments expressed in HeLa cells and translation intermediates synthesized in reticulocyte lysate, the results obtained with Hdj-2 are supportive of each other. However, in these different experimental systems we observed differences in our ability to co-immunoprecipitate CFTR with Hdj-1. In the HeLa cell expression system, compared with Hsc70 and Hdj-2, low levels of CFTR fragments were co-precipitated with Hdj-1. In contrast, levels of complexes between Hdj-1 and CFTR translation intermediates generated in reticulocyte lysates were nearly equivalent to those isolated with Hsc70 and Hdj-2. Similar to Hdj-2, Hdj-1 binding was enhanced by the expression of cytosolic regions of CFTR, however it did not appear sensitive to ATP depletion, nor was it markedly reduced by expression of the R-domain. Binding of Hdj-1 and Hdj-2 to CFTR translation intermediates therefore does not appear to occur at the same sites. At present we are unable to ascribe a functional role for Hdj-1 in CFTR folding. However, Hdj-1 has been observed to bind extended regions of nascent chains as they emerge from ribosomes to promote their subsequent folding (Frydman *et al*., 1994). Perhaps Hdj-1 plays a similar role in CFTR biogenesis.

Mechanistic data which show that purified Hdj-2, but not Hdj-1, can function independently to suppress the aggregation of purified NBD1 help explain why we observe differences in their ability to interact with CFTR biogenic intermediates. These data suggest that Hdj-2 is much more effective than Hdj-1 at binding NBD1. Hdj-2 therefore appears better suited than Hdj-1 at facilitating aspects of CFTR assembly which involve NBD1. Insight into why these Hsp40 proteins are not functionally equivalent comes from examination of their domain structure. Hdj-2 contains a the zinc finger-like region and the conserved C-terminus of *E.coli* DnaJ (Chellaiah *et al*., 1993), whereas Hdj-1 lacks the zinc finger-like domain (Ohtsuka, 1993). Hsp40 proteins which contain a zinc finger-like domain and the conserved C-terminus function as chaperones with high efficiency. Whereas Hsp40s that contain only the conserved C-terminus function as polypeptide binding proteins, but when compared with their zinc finger-containing counter parts, exhibit differences in substrate specificity and protein folding activity (Banecki *et al*., 1996; Szabo *et al*., 1996; Terada *et al*., 1997; Lu and Cyr, 1998b).

Another factor that appears to enhance the ability of Hdj-2 to bind CFTR translation intermediates is its localization to the ER surface. Membrane-localized Hdj-2 is positioned on the ER surface where it can bind cytosolic regions of membrane proteins during or soon after their synthesis. The presence of a farnesyl tail on Hdj-2 appears to contribute to its membrane localization (Caplan *et al*., 1992). Farnesylation of Hdj-2 may increase the efficiency of its chaperone action by limiting its diffusion away from membrane proteins during cycles of polypeptide binding and release that are required for it promote their folding/assembly. The localization of an Hsp40 co-chaperone to the ER surface appears to provide a cellular mechanism to recruit Hsc70 from the cytosol to facilitate early stages in membrane protein biogenesis. We are currently investigating whether the Hdj-2/Hsc70 chaperone pair is a general component of the cellular machinery which facilitates the biogenesis of membrane proteins that expose large domains in the cytosol.

Materials and methods

Antibodies

Antibodies utilized in this study were acquired from the following sources: rabbit polyclonal α-Hdj-1 (#SPA-400), rat monoclonal α-Hsc70 (#SPA-815), rabbit polyclonal α-Tcp-1 (#CTA-200) and rabbit polyclonal α-calnexin (#SPA-860) were from StressGen Biotechnologies. Mouse monoclonal Hdj-2 (# MS-225) was from Neomarkers and mouse monoclonal α-calnexin (MA3-027) was from Affinity Bioreagents. α-CFTR was generated against a GST fusion protein that contained residues 1–79 of CFTR and was a gift from Dr Kevin Kirk in the Physiology and Biophysics Department at UAB. Goat anti-rabbit IgG–Oregon Green and goat anti-mouse IgG–Texas Red (Molecular Probes) conjugates were utilized as secondary antibodies in indirect immunofluorescence experiments. Western blot analysis indicated that the aforementioned antibodies were mono-specific for the indicated proteins present in the cultured cells (Figure 2) and reticulocyte lysates (data not shown).

Indirect immunofluorescence

Pancreatic carcinoma cells (CFPAC-1; Schoumacher *et al*., 1990) were cultured on cover slips in Dulbecco's modified Eagle's medium (DMEM; Cellgro) which was supplemented with 10% FBS (Hyclone) and 10% bovine serum albumin (BSA) at 37°C in an atmosphere of 5% CO_2. Cells were fixed at 80% confluence with ice-cold absolute methanol. Antibodies were diluted in phosphate-buffered saline (PBS) containing 1.0% BSA. To localize Hdj-1, coverslips were decorated with a mixture of rabbit polyclonal α-Hdj-1 (1:100 dilution) and mouse monoclonal α-calnexin (1:100 dilution). Hdj-2 was localized by incubating coverslips with mouse monoclonal α-Hdj-2 (1:100 dilution) and rabbit polyclonal α-calnexin (1:100 dilution). Incubations with the respective primary antibodies were carried out for 40 min at 37°C. Coverslips were washed three times with PBS–0.1% BSA and then decorated with a mixture of goat anti-mouse IgG–Texas Red and goat anti-rabbit IgG–Oregon Green. Indirect immunofluorescent patterns attributed to the respective chaperone proteins were visualized in 0.5 μM sections of cells by digital confocal microscopy utilizing an Olympus IX70 epifluorescence microscope equipped with a step motor. Optical sections were captured with a CCD high resolution video camera equipped with a camera/computer interface. Images were then analyzed with a PowerMac 9500/132 computer utilizing IP Lab Spectrum software (Signal Analytics).

Construction of CFTR expression vectors

pCDNA-CFTR and pCDNA-ΔF508 CFTR expression plasmids were constructed by subcloning a *Not*I–*Xho*I fragment excised from pBQ4.7 (Riordan *et al*., 1989) that contained the respective open reading frames (ORFs) into the multiple cloning site of pCDNA3.1(+) (Invitrogen).

To express different length CFTR fragments in HeLa cells, PCR-directed mutagenesis was utilized to introduce stop codons at different locations in the CFTR ORF in pTM1-CFTR (Gregory *et al*., 1990). This was accomplished by excising a fragment from pTM1-CFTR and replacing it with a smaller PCR product containing the authentic sequence up to an engineered stop codon at the 3′ end. pTM1-CFTR 370X, pTM1-CFTR 593X and pTM1-CFTR 893X were all generated using this strategy. For pTM1-CFTR 370X, a 4 kb *Xba*I–*Pst*I fragment was excised from pTM1-CFTR and replaced with a 580 bp *Xba*I–*Pst*I PCR fragment containing a stop codon after residue 370. pTM1-CFTR 593X was constructed in a similar fashion: a 3 kb *Sph*I–*Pst*I fragment was removed from pTM1-CFTR and replaced with a 240 bp *Sph*I–*Pst*I PCR fragment which contained a stop codon after residue 593. The pTM1-CFTR 837X plasmid was generated by substituting a 3 kb *Sph*I–*Stu*I fragment in pTM1-CFTR for a 1060 bp *Sph*I–*Stu*I PCR fragment that contained a stop codon after residue 837. The last expression vector, pTM1-CFTR 1162X, was made by replacing an *Nco*I–*Est*107I fragment from pTM1-CFTR with a 2357 bp *Nco*I–*Est*1107I fragment from pDB480 that contained a natural stop mutation after residue 1162.

For *in vitro* expression in reticulocyte lysates (see below), three constructs were made that, when linearized, would generate truncated mRNAs encoding CFTR translation intermediates of different sizes. The translation intermediates were truncated before the natural glycosylation site present in MSDII, so a glycosylation site was engineered into the third extracellular loop (EL3) of CFTR to monitor membrane insertion. This was accomplished by replacing a *Xba*I–*Sph*I fragment from pTM1-CFTR with a *Xba*I–*Sph*I fragment that contained the EL3 glycosylation site from pNUT-EL3-CFTR (provided by Dr Riordan of the Mayo Clinic at Scottsdale, AZ; Chang *et al*., 1994) thus generating pTM1-EL3-CFTR. CFTR truncations at residues 430 and 897 were made by linearizing the pTM1-CFTR expression vector at a restriction site engineered immediately after the indicated amino acid residue. Thus, for pTM1-CFTR 430, a 1050 bp *Xba*I–*Sph*I fragment was removed from pTM1-EL3-CFTR and replaced with a 750 bp *Xba*I–*Sph*I PCR fragment, and for pTM1-CFTR 897, a 1310 bp *Hpa*I–*Bgl*II fragment was removed from pTM1-EL3-CFTR and replaced with a 350 bp *Hpa*I–*Bgl*II PCR fragment. When linearized with *Sph*I or *Bgl*II respectively, pTM1-CFTR 430 and pTM1-CFTR 897 express CFTR truncations that terminate at residue 430 or 897.

Co-immunoprecipitation of CFTR expressed in HeLa cells with chaperone proteins

HeLa (CCL-2; ATCC) cells were grown in 6-well trays (35 mm/well) at 37°C/5% CO_2 in DMEM supplemented with 10% FBS and 1% PenStrep to 70% confluency. Cells were then incubated with 0.25 μg of expression vector dissolved in DOTAP:DOPE (Avanti Polar Lipids) which was delivered in a volume of 0.7 ml. Cells were then infected with recombinant vaccinia virus (m.o.i. = 1) expressing T_7 polymerase (vTF7.3; Fuerst *et al*., 1986). After an 8 h incubation at 37°C/5% CO_2, cells were rinsed with 0.7 ml PBS and incubated in 0.7 ml of methionine-free MEM (Gibco-BRL) for 30 min. Tran^{35}S-label (100 μCi/well; 1200 Ci/mmol; ICN Radiochemicals) was then added in a volume of 350 μl in methionine-free MEM and the cells were incubated for the indicated times. Cells were lysed under non-denaturing conditions with 250 μl of buffer A: PBS (pH 7.4) supplemented with 0.1% Triton X-100, 5 mM Mg-ATP, 80 mM phosphocreatine, 500 μg/ml creatine phosphokinase and 100 μg/ml Pefabloc SC (Boehringer Mannheim). To remove radiolabeled material which adheres non-specifically to PG (Boehringer Mannheim), cell lysates were treated immediately with Pansorbin (2%; Calbiochem) for 15 min at 0°C. Pansorbin and other insoluble material were then pelleted by centrifugation at 20 000 *g* for 5 min at 4°C and supernatants were collected and assayed for protein concentration (Bradford method; Bio-Rad) using BSA as a standard. Co-immunoprecipitation reactions containing 12.5 μg of total lysate protein and antisera specific for Hsc70 (12.5 μg), Hdj-1 (0.5 μg), Hdj-2 (5 μg), Tcp-1 (2.5 μg), CFTR (2.5 μg) or mouse IgG (1.0 μg) were then carried out in a final volume of 65 μl. These quantities of antibody were chosen because they were shown to immunoprecipitate the majority of the chaperone of interest from cell lysates (Figure 2A). Reactions were incubated for 30 min at 0°C followed by the addition of 25 μl of a 70% slurry of PG and a second 30 min incubation. Samples were then washed once with 0.6 ml of buffer A and proteins that adhered to the protein G pellets were prepared for gel analysis by incubation in 2× SDS sample buffer for 10 min at 50°C. Significant levels of CFTR were not precipitated with Hsp70, Hdj-1, Hdj-2 or Tcp-1 antisera under denaturing conditions (data not shown). Due to a dilution of the cellular environment, complexes between substrate proteins and Hsp70 or Hsp40 proteins in cell lysates are unstable and tend to dissociate. However, the levels of complexes isolated between Hsp70 and Hsp40 proteins with CFTR are in the range of those reported in the literature with other proteins (Ungermann *et al*., 1994, 1996).

To carry out re-immunoprecipitations protein G–agarose pellets isolated in the co-immunoprecipitation reactions were resuspended in 25 μl of 2× SDS–PAGE sample buffer and then incubated for 10 min at 50°C. Samples were mixed and then a 20 μl aliquot was diluted to 750 μl with PBS supplemented with 0.1% Triton X-100, 0.1% SDS and 0.5% BSA. Then 2.5 μg α-CFTR mouse polyclonal antisera raised against the N-terminus of CFTR was added. Incubations were then carried out for 45 min at room temperature. A 50 μl aliquot of a 50% slurry of protein A–Sepharose in the above buffer was then added and incubations were extended for an additional 45 min. Samples were then spun in a centrifuge and protein A–Sepharose pellets were washed two times in PBS supplemented 0.1% Triton X-100 and 0.1% SDS. To elute immunoprecipitated material from the pelleted beads 20 ml of 1× SDS sample buffer was added and a 20 min of incubation at 50°C was carried out. Eluted material was then analyzed by SDS–PAGE and fluorography.

In vitro transcription/translation of CFTR and characterization of the CFTR translation product

Cell-free protein synthesis was performed using a rabbit reticulocyte-coupled transcription/translation system supplemented with canine pancreatic microsomes as recommended by the manufacturer (Promega). To determine if Hsp70, Hdj-1 or Hdj-2 bind CFTR co-translationally, co-immunoprecipitations of ribosome-bound CFTR translation intermediates with the aforementioned chaperone proteins was performed (see below). Lysates were programmed with CFTR expression vectors linearized before the stop codon yielding truncated mRNA encoding translation intermediates that remain ribosome-bound. CFTR translation intermediates truncated at residues 430 or 897 were generated by programming lysates with 0.35 μg of pTM1-CFTR 430 linearized with *Sph*I or 0.035 μg of pTM1-CFTR 897 linearized with *Bgl*II respectively. A CFTR truncation at residue 776 was made by programming reticulocyte lysates with 0.035 μg of pTM1-EL3-CFTR linearized with *Hpa*I. *In vitro* transcription/translation reactions were carried out for 60 min at 30°C in a volume of 50 μl. Translations were then terminated with cycloheximide (20 μg/ml) and placed on ice.

To assess the efficiency of insertion of *in vitro* synthesized CFTR into microsomes, EndoH treatment and sodium carbonate extraction were performed. For EndoH treatment, two 10 μl aliquots of a translation reaction were each diluted in half with buffer B (0.1% Triton X-100, 0.05% BSA and 100 mM sodium citrate pH 5.5). EndoH (0.25 U; Boehringer Mannheim) was added to one aliquot and buffer B to the other. Both were then incubated for 2 h at 30°C, followed by the addition of 2× SDS sample buffer. For carbonate extraction, a 10 μl aliquot of a translation reaction was diluted in half with 200 mM sodium carbonate pH 11.0 and incubated at 0°C for 30 min. Then, 130 μl of

buffer C (80 mM KCl, 20 mM Tris–Cl, pH 8.0) was added and the reaction was placed on a 50 µl 0.5 M sucrose cushion. The sample was then centrifuged for 10 min at 60 000 *g* at 4°C in a Beckman TLA100.1 rotor. The pellet was immediately solubilized in SDS sample buffer and the supernatant was precipitated with ice-cold 80% acetone. Precipitates were then isolated by centrifugation and solubilized in SDS sample buffer. Samples were then incubated at 50°C for 10 min and analyzed by SDS–PAGE.

Co-immunoprecipitation of CFTR in vitro translation products with chaperone proteins

CFTR translation products (10 µl) were diluted 10-fold into buffer D containing 80 mM KCl, 20 mM HEPES pH 7.4, 1.5 mM $MgCl_2$, 0.05% BSA, 0.1% Triton X-100 and 10 µg/ml Pefabloc SC. Where indicated, 0.25 U/µl apyrase (Sigma Chemical Co.) was included in buffer D to reduce ATP levels (Cyr *et al*., 1993). Antisera specific for Hsc70 (10 µg), Hdj-1 (1 µg), or Hdj-2 (2.5 µg) was then added to the reaction to initiate co-immunoprecipitation reactions and complexes were isolated with PG (Ungermann *et al*., 1996).

Purification of Hsp70, Hdj-1 and Hdj-2

Hsp70 was expressed from pET11A-Hsp70 in *E.coli* strain BL21(DE3) and purified by standard techniques (Cyr *et al*., 1992; Freeman *et al*., 1995). Hdj-1 was overexpressed in *E.coli* from pET21D-HDJ1 (Freeman *et al*., 1995) and purified as follows: cells from a 500 ml culture were harvested after a 3 h induction period with 0.5 mM IPTG and lysed by sonication in buffer 1 [10 mM HEPES pH 7.0, 20 mM NaCl, 0.5 mM EDTA, 2 mM dithiothreitol (DTT), 0.5 mM phenylmethyl sulfonyl fluoride]. The high speed supernatant was loaded onto a 15 ml mono-Q ion column equilibrated with buffer 1. Approximately 60% of the Hdj-1 present in the lysate was retained by this column and the remainder was found in the flow through. Bound Hdj-1 was eluted by increasing NaCl from 20–60 mM. Protein eluted in this step was ~85% pure and further purified by hydroxylapatite chromatography (Cyr *et al*., 1992).

pET9D-Hdj-2 was constructed to overexpress Hdj-2 in *E.coli* strain Bl21(DE3) as described above. Hdj-2 present in the high-speed supernatant of cell lysates was purified by mono-Q and hydroxylapatite chromatography as previously described for the yeast Hsp40 protein Ydj1 (Cyr *et al*., 1992; Cyr and Douglas, 1994).

After the final purification step Hdj-1, Hdj-2 and Hsp70 were dialyzed against 20 mM HEPES pH 7.4, 150 mM NaCl, 2 mM DTT and 5% glycerol and concentrated to 1.0 mg/ml. Aliquots of proteins were then snap-frozen in liquid nitrogen and stored at –80°C until used. Protein concentrations were estimated with BSA as the standard utilizing the Bio-Rad Bradford reagent.

Assay for Hsp70 ATPase activity

Hdj-1 or Hdj-2 were assayed for their ability to stimulate Hsp70 ATPase activity by thin layer chromatography on PEI cellulose plates utilizing standard assay conditions (Cyr *et al*., 1992). Spontaneous ADP formation was assayed and subtracted prior to calculations for rates of ATP hydrolysis.

Measurement of NBD1 aggregation

NBD1 was over-expressed in *E.coli* and was purified from inclusion bodies according to a the published protocol of the laboratory of Dr Phil Thomas at the University of Texas Southwestern Medical Center (Qu *et al*., 1997). Prior to assay for aggregation, stocks of NBD1 were diluted to a concentration of 50 µM in 6 M guanidinium–HCl which was buffered with 20 mM HEPES pH 7.2, 50 mM KCl and 10 mM DTT. After incubation in this buffer for 1 h at 30°C, NBD1 was diluted 100-fold into 250 µl of folding buffer (20 mM HEPES pH 7.2, 50 mM KCl, 2 mM $MgCl_2$ and 1 mM ATP) that was contained in a water jacketed cuvette. Aggregation of NBD1 was then monitored over time at 30°C by measuring increases in light scattering at 320 nm. Where indicated, chaperone proteins were added at the indicated concentrations to reaction mixtures prior to the addition of NBD1. In some cases, $MgCl_2$ and ATP were omitted from the reactions.

Acknowledgements

The authors thank Richard Morimoto for pET-Hsc70 and pET-Hdj-1 expression vectors; Phil Thomas for the NBD1 expression plasmid; David Bedwell and Kevin Kirk for α-CFTR sera; Jim Collawn and Margaret Scully for critical reading of the manuscript. This work was supported by a Research Grant from the Cystic Fibrosis Foundation, a Grant in Aid from the Alabama Affiliate of the American Heart Association and R01GM56981 from the National Institutes of Health.

References

Anderson,M.P., Gregory,R.J., Thompson,S., Souza,D.W., Paul,S., Mulligan,R.C., Smith,A.E. and Welsh,M.J. (1991) Demonstration that CFTR is a chloride channel by alteration of its anion selectivity. *Science*, **253**, 202–205.

Banecki,B., Liberek,K., Wall,D., Wawrzynow,A., Georgopoulos,C., Bertoli,E., Tanfani,F. and Zylicz,M. (1996) Structure–function analysis of the zinc finger region of the DnaJ molecular chaperone. *J. Biol. Chem.*, **271**, 14840–14848.

Brodsky,J.L., Hamamoto,S., Feldheim,D. and Schekman,R. (1993) Reconstitution of protein translocation from solubilized yeast membranes reveals topologically distinct roles for BiP and cytosolic Hsc70. *J. Cell Biol.*, **120**, 95–102.

Brown,C.R., Hong-Brown,L.Q., Biwersi,J., Verkman,A.S. and Welch,W.J. (1996) Chemical chaperones correct the mutant phenotype of the DF508 cystic fibrosis transmembrane conductance regulator protein. *Cell Stress Chaper.*, **1**, 117–125.

Caplan,A.J., Tsai,J., Casey,P.J. and Douglas,M.G. (1992) Farnesylation of YDJ1p is required for function at elevated growth temperatures in *Saccharomyces cerevisiae*. *J. Biol. Chem.*, **267**, 18890–18895.

Caplan,A.J., Cyr,D.M. and Douglas,M.G. (1993) Eukaryotic homologues of *Escherichia coli* dnaJ: a diverse protein family that functions with hsp70 stress proteins. *Mol. Biol. Cell*, **4**, 555–563.

Chang,X.B., Hou,Y.X., Jensen,T.J. and Riordan,J.R. (1994) Mapping of cystic fibrosis transmembrane conductance regulator membrane topology by glycosylation site insertion. *J. Biol. Chem.*, **269**, 18572–18575.

Chellaiah,A., Davis,A. and Mohanakumar,T. (1993) Cloning of a unique human homologue of the *Escherichia coli* DnaJ heat shock protein. *Biochim. Biophys. Acta*, **1174**, 111–113.

Cyr,D.M. (1997) The Hsp40 (DnaJ-related) family of proteins. In Gething,M.J. (ed.), *Guidebook to Molecular Chaperones and Protein Folding Factors*. Sambrook & Tooze at Oxford University Press, Oxford, UK, pp. 89–95.

Cyr,D.M. and Douglas,M.G. (1994) Differential regulation of Hsp70 subfamilies by the eukaryotic DnaJ homologue YDJ1. *J. Biol. Chem.*, **269**, 9798–9804.

Cyr,D.M. and Neupert,W. (1996) Roles for Hsp70 protein in intracellular protein transport. In Feige,U., Morimoto,R., Yahara,I. and Polla,B. (eds), Stress-Inducible Cellular Responses. Birkhauser/Springer, pp. 25–40.

Cyr,D.M., Lu,X. and Douglas,M.G. (1992) Regulation of Hsp70 function by a eukaryotic DnaJ homolog. *J. Biol. Chem.*, **267**, 20927–20931.

Cyr,D.M., Stuart,R.A. and Neupert,W. (1993) A matrix ATP requirement for presequence translocation across the inner membrane of mitochondria. *J. Biol. Chem.*, **268**, 23751–23754.

Cyr,D.M., Langer,T. and Douglas,M.G. (1994) DnaJ-like proteins: molecular chaperones and specific regulators of Hsp70. *Trends Biochem. Sci.*, **19**, 176–181.

Denning,G.M., Anderson,M.P., Amara,J.F., Marshall,J., Smith,A.E. and Welsh,M.J. (1992) Processing of mutant cystic fibrosis transmembrane conductance regulator is temperature-sensitive. *Nature*, **358**, 761–764.

Devuyst,O., Burrow,C.R., Schwiebert,E.M., Guggino,W.B. and Wilson,P.D. (1996) Developmental regulation of CFTR expression during human nephrogenesis. *Am. J. Physiol.*, **271**, 723–735.

Fedorov,A.N. and Baldwin,T.O. (1997) Co-translational protein folding. *J. Biol. Chem.*, **272**, 32715–32718.

Freeman,B.C., Myers,M.P., Schumacher,R. and Morimoto,R.I. (1995) Identification of a regulatory motif in Hsp70 that affects ATPase activity, substrate binding and interaction with HDJ1. *EMBO J.*, **14**, 2281–2292.

Frydman,J. and Hohfeld,J. (1997) Chaperones get in touch: the Hip–Hop connection. *Trends Biochem. Sci.*, **22**, 87–92.

Frydman,J., Nimmesgern,E., Ohtsuka,K. and Hartl,F.U. (1994) Folding of nascent polypeptide chains in a high molecular mass assembly with molecular chaperones. *Nature*, **370**, 111–117.

Fuerst,T.R., Niles,E.G., Studier,F.W. and Moss,B. (1986) Eukaryotic transient-expression system based on recombinant vaccinia virus that synthesizes bacteriophage T7 RNA polymerase. *Proc. Natl Acad. Sci. USA*, **83**, 8122–8126.

Gasparini,P., Borgo,G., Mastella,G., Bonizzato,A., Dognini,M. and Pignatti,P.F. (1992) Nine cystic fibrosis patients homozygous for the

CFTR nonsense mutation R1162X have mild or moderate lung disease. *J. Med. Genet.*, **29**, 558–562.
Gaut,J.R. and Hendershot,L.M. (1993) The modification and assembly of proteins in the endoplasmic reticulum. *Curr. Opin. Cell Biol.*, **5**, 589–595.
Georgopoulos,C.P., Lundquist-Heil,A., Yochem,J. and Feiss,M. (1980) Identification of the *E.coli* dnaJ gene product. *J. Mol. Gen. Genet.*, **178**, 583–588.
Gregory,R.J. *et al.* (1990) Expression and characterization of the cystic fibrosis transmembrane conductance regulator. *Nature*, **347**, 382–386.
Hartl,F.U. (1996) Molecular chaperones in cellular protein folding. *Nature*, **381**, 571–579.
Higgins,C.F. (1992) ABC transporters: from microorganisms to man. *Annu. Rev. Cell Biol.*, **8**, 67–113.
Hohfeld,J. and Jentsch,S. (1997) Grpe-Like regulation of the Hsc70 chaperone by the anti-apoptotic protein Bag-1. *EMBO J.*, **16**, 6209–6216.
Hurtley,S.M. and Helenius,A. (1989) Protein oligomerization in the endoplasmic reticulum. *Annu. Rev. Cell Biol.*, **5**, 277–307.
Jensen,T.J., Loo,M.A., Pind,S., Williams,D.B., Goldberg,A.L. and Riordan,J.R. (1995) Multiple proteolytic systems, including the proteasome, contribute to CFTR processing. *Cell*, **83**, 129–135.
Langer,T., Lu,C., Echols,H., Flanagan,J., Hayer,M.K. and Hartl,F.U. (1992) Successive action of DnaK, DnaJ and GroEL along the pathway of chaperone-mediated protein folding. *Nature*, **356**, 683–689.
Liberek,K., Marszalek,J., Ang,D., Georgopoulos,C. and Zylicz,M. (1991) *Escherichia coli* DnaJ and GrpE heat shock proteins jointly stimulate ATPase activity of DnaK. *Proc. Natl Acad. Sci. USA*, **88**, 2874–2878.
Lu,Y., Xiong,X.M., Helm,A., Kimani,K., Bragin,A. and Skach,W.R. (1998) Co- and post-translational translocation mechanisms direct cystic fibrosis transmembrane conductance regulator N terminus transmembrane assembly. *J. Biol. Chem.*, **273**, 568–576.
Lu,Z. and Cyr,D.M. (1998a) The conserved carboxyl terminus and zinc finger-like domain of the co-chaperone Ydj1 assist Hsp70 in protein folding. *J. Biol. Chem.*, **273**, 5970–5978.
Lu,Z. and Cyr,D.M. (1998b) Protein folding activity of Hsp70 is modified differentially by the Hsp40 co-chaperones Sis1 and Ydj1. *J. Biol. Chem.*, **273**, 27824–27830.
Lukacs,G.L., Mohamed,A., Kartner,N., Chang,X.B., Riordan,J.R. and Grinstein,S. (1994) Conformational maturation of CFTR but not its mutant counterpart (DF508) occurs in the endoplasmic reticulum and requires ATP. *EMBO J.*, **13**, 6076–6086.
Minami,Y., Hohfeld,J., Ohtsuka,K. and Hartl,F.U. (1996) Regulation of the heat-shock protein 70 reaction cycle by the mammalian DnaJ homolog, Hsp40. *J. Biol. Chem.*, **271**, 19617–19624.
Netzer,W.J. and Hartl,F.U. (1997) Recombination of protein domains facilitated by co-translational folding in eukaryotes. *Nature*, **388**, 343–349.
Ohtsuka,K. (1993) Cloning of a cDNA for heat-shock protein hsp40, a human homologue of bacterial DnaJ. *Biochem. Biophys. Res. Commun.*, **197**, 235–240.
Ostedgaard,L.S., Rich,D.P., DeBerg,L.G. and Welsh,M.J. (1997) Association of domains within the cystic fibrosis transmembrane conductance regulator. *Biochemistry*, **36**, 1287–1294.
Pasyk,E.A. and Foskett,J.K. (1995) Mutant (delta F508) cystic fibrosis transmembrane conductance regulator Cl-channel is functional when retained in endoplasmic reticulum of mammalian cells. *J. Biol. Chem.*, **270**, 12347–12350.
Perara,E., Rothman,R.E. and Lingappa,V.R. (1986) Uncoupling translocation from translation: implications for transport of proteins across membranes. *Science*, **232**, 348–352.
Pind,S., Riordan,J.R. and Williams,D.B. (1994) Participation of the endoplasmic reticulum chaperone calnexin (p88, IP90) in the biogenesis of the cystic fibrosis transmembrane conductance regulator. *J. Biol. Chem.*, **269**, 12784–12788.
Qu,B.H., Strickland,E.H. and Thomas,P.J. (1997) Localization and suppression of a kinetic defect in cystic fibrosis transmembrane conductance regulator folding. *J. Biol. Chem.*, **272**, 15739–15744.
Riordan,J.R. *et al.* (1989) Identification of the cystic fibrosis gene: cloning and characterization of complementary DNA. *Science*, **245**, 1066–1073.
Sato,S., Ward,C.L., Krouse,M.E., Wine,J.J. and Kopito,R.R. (1996) Glycerol reverses the misfolding phenotype of the most common cystic fibrosis mutation. *J. Biol. Chem.*, **271**, 635–638.
Schoumacher,R.A. *et al.* (1990) A cystic fibrosis pancreatic adenocarcinoma cell line. *Proc. Natl Acad. Sci. USA*, **87**, 4012–4016.
Schwiebert,E.M., Morales,M.M., Devidas,S., Egan,M.E. and Guggino,W.B. (1998) Chloride channel and chloride conductance regulator domains of CFTR, the cystic fibrosis transmembrane conductance regulator. *Proc. Natl Acad. Sci. USA*, **95**, 2674–2679.
Sheppard,D.N., Ostedgaard,L.S., Rich,D.P. and Welsh,M.J. (1994b) The amino-terminal portion of CFTR forms a regulated Cl-channel. *Cell*, **76**, 1091–1098.
Silver,P.A. and Way,J.C. (1993) Eukaryotic DnaJ homologs and the specificity of Hsp70 activity. *Cell*, **74**, 5–6.
Strickland,E., Qu,B.H., Millen,L. and Thomas,P.J. (1997) The molecular chaperone Hsc70 assists the *in vitro* folding of the N-terminal nucleotide-binding domain of the cystic fibrosis transmembrane conductance regulator. *J. Biol. Chem.*, **272**, 25421–25424.
Szabo,A., Korszun,R., Hartl,F.U. and Flanagan,J. (1996) A zinc finger-like domain of the molecular chaperone DnaJ is involved in binding to denatured protein substrates. *EMBO J.*, **15**, 408–417.
Takayama,S., Bimston,D.N., Matsuzawa,S., Freeman,B.C., Aime-Sempe,C., Xie,Z., Morimoto,R.I. and Reed,J.C. (1997) BAG-1 modulates the chaperone activity of Hsp70/Hsc70. *EMBO J.*, **16**, 4887–4896.
Terada,K., Kanazawa,M., Bukau,B. and Mori,M. (1997) The human DnaJ homologue dj2 facilitates mitochondrial protein import and luciferase refolding. *J. Cell Biol.*, **139**, 1089–1095.
Ungermann,C., Neupert,W. and Cyr,D.M. (1994) The role of Hsp70 in conferring unidirectionality on protein translocation into mitochondria. *Science*, **266**, 1250–1253.
Ungermann,C., Guiard,B., Neupert,W. and Cyr,D.M. (1996) The membrane potential and Hsp70/MIM44-dependent reaction cycle driving early steps of protein import into mitochondria. *EMBO J.*, **15**, 735–744.
Ward,C.L. and Kopito,R.R. (1994) Intracellular turnover of cystic fibrosis transmembrane conductance regulator. Inefficient processing and rapid degradation of wild-type and mutant proteins. *J. Biol. Chem.*, **269**, 25710–25718.
Ward,C.L., Omura,S. and Kopito,R.R. (1995) Degradation of CFTR by the ubiquitin–proteasome pathway. *Cell*, **83**, 121–127.
Welsh,M.J. and Ostedgaard,L.S. (1998) Cystic fibrosis problem probed by proteolysis. *Nature Struct. Biol.*, **5**, 167–169.
Welsh,M.J. and Smith,A.E. (1993) Molecular mechanisms of CFTR chloride channel dysfunction in cystic fibrosis. *Cell*, **73**, 1251–1254.
Wickner,S., Hoskins,J. and McKenney,K. (1991) Function of DnaJ and DnaK as chaperones in origin-specific DNA binding by RepA. *Nature*, **350**, 165–167.
Winter,M.C. and Welsh,M.J. (1997) Stimulation of CFTR activity by its phosphorylated R domain. *Nature*, **389**, 294–296.
Xiong,X., Bragin,A., Widdicombe,J.H., Cohn,J. and Skach,W.R. (1997) Structural cues involved in endoplasmic reticulum degradation of G85E and G91R mutant cystic fibrosis transmembrane conductance regulator. *J. Clin. Invest.*, **100**, 1079–1088.
Yang,Y., Janich,S., Cohn,J.A. and Wilson,J.M. (1993) The common variant of cystic fibrosis transmembrane conductance regulator is recognized by hsp70 and degraded in a pre-Golgi nonlysosomal compartment. *Proc. Natl Acad. Sci. USA*, **90**, 9480–9484.
Zhang,F.L. and Casey,P.J. (1996) Protein prenylation: molecular mechanisms and functional consequences. *Annu. Rev. Biochem.*, **65**, 241–269.
Zhang,F., Kartner,N. and Lukacs,G.L. (1998) Limited proteolysis as a probe for arrested conformational maturation of DF508 CFTR. *Nature Struct. Biol.*, **5**, 180–183.
Zylicz,M., Yamamoto,T., McKittrick,N., Sell,S. and Georgopoulos,C. (1985) Purification and properties of the dnaJ replication protein of *Escherichia coli*. *J. Biol. Chem.*, **260**, 7591–7598.

Received February 13, 1998; revised and accepted January 19, 1999